Annals of Gastroenterology (2015) **28,** 193-202

Recent developments in imaging of pancreatic neuroendocrine tumors

Nikolaos Kartalis[a,b], Raffaella Maria Pozzi Mucelli[a,b], Anders Sundin[c]

Karolinska Institutet, Stockholm; Karolinska University Hospital, Stockholm; Uppsala University, Uppsala, Sweden

Abstract

Pancreatic neuroendocrine tumors (PNETs) are very rare, accounting for 1-2% of all pancreatic neoplasms. They are classified into functioning and non-functioning and their behavior varies widely from benign to highly malignant. For their investigation, a variety of anatomical and functional imaging methods are available. Anatomical methods include computed tomography (CT), magnetic resonance imaging, and ultrasonography. Functional methods include scintigraphy and positron emission tomography (PET). A combination of anatomical and morphological methods results in the so-called hybrid imaging, such as PET/CT. We herein discuss the currently available imaging modalities for the investigation of PNETs and, more specifically, their applications in tumor detection and staging as well as in choice of therapy, imaging follow up and prediction of response, with emphasis on the recent developments.

Keywords Anatomical imaging, functional imaging, pancreatic neoplasms

Ann Gastroenterol 2015; 28 (2): 193-202

Introduction

Pancreatic neuroendocrine tumors (PNETs) are rare (incidence 1/100,000 x year) and account for about 1-2% of all pancreatic neoplasias [1,2]. They are, in the majority of cases, sporadic but may also be part of various syndromes, such as multiple endocrine neoplasia 1, von Hippel-Lindau's disease, tuberous sclerosis, and neurofibromatosis [3-5].

Based on the presence or absence of symptoms related to hormone production, PNETs are classified into functioning and non-functioning, respectively. Non-functioning tumors may, however, secret hormones that can be detected biochemically [6,7].

The clinical behavior of PNETs varies widely from benign to highly malignant neoplasms. For their grading, the WHO-2010 system classifies them into well-differentiated (grade 1, G1; and grade 2, G2) and poorly differentiated (grade 3, G3) tumors, based on their ki-67 labeling index and mitotic count (Table 1) [8]. Presently, staging of PNETs is performed separately from grading, as opposed to the WHO-2004 classification system. The staging protocol proposed from the European Neuroendocrine Tumor Society (ENETS) is widely accepted and reproducible (Table 2) [9,10]. Most of PNETs express somatostatin receptors (SSR), which are of interest for both diagnostic and therapeutic purposes.

Surgery is regarded as the only curative treatment but, unfortunately, cannot be offered to more than 50% of the patients due to locally advanced or disseminated disease [11]. However, surgery can be additionally performed with non-curative intention, i.e. for debulking of the primary tumor and/or metastases to alleviate symptoms. Treatment of liver metastases may be achieved by locoablative procedures, such as radiofrequency/microwave ablation and transarterial embolization with or without chemotherapeutic or radioactive substances. Systemic treatments, such as chemotherapy, inhibitors of mTOR (everolimus), tyrosine kinase (sunitinib), and unlabeled (cold) and radiolabeled somatostatin analogs (SSA), are currently available in patients with inoperable and/or metastatic disease [12,13]. Treatment with radiolabeled SSA,

Table 1 Grading of pancreatic neuroendocrine tumors according to the WHO-2010 classification system [8]

	Well-differentiated (NET)		Poorly-differentiated (NEC)
Tumor grade	1	2	3
Ki-67 index (%)	<3	3-20	>20
Mitotic count (per 10 HPF)	<2	2-20	>20

WHO, World Health Organization; NET, neuroendocrine tumor; NEC, neuroendocrine carcinoma; HPF, high-power field

[a]Division of Medical Imaging and Technology, Department of Clinical Science, Intervention and Technology (CLINTEC), Karolinska Institutet, Stockholm (Nikolaos Kartalis, Raffaella Maria Pozzi Mucelli); [b]Department of Radiology, Karolinska University Hospital, Stockholm (Nikolaos Kartalis, Raffaella Maria Pozzi Mucelli); [c]Department of Radiology, Oncology and Radiation Sciences, Uppsala University, Uppsala (Anders Sundin), Sweden

Conflict of Interest: None

Correspondence to: Nikolaos Kartalis, C1-46, KS Huddinge, 14186, Stockholm, Sweden, Tel.: + 46 858 584628, e-mail address: nikolaos.kartalis@karolinska.se

Received 05 July 2014; accepted 27 August 2014

Table 2 Staging protocol of pancreatic neuroendocrine tumors, as proposed by the European Neuroendocrine Tumor Society [10]

T-stage	
TX	Primary tumor cannot be assessed
T0	No evidence of primary tumor
T1	Tumor confined to pancreas, <2 cm
T2	Tumor confined to pancreas, 2-4 cm
	Tumor confined to pancreas, >4 cm or
T3	Invades duodenum or bile duct
T4	Tumor invades adjacent organs or major vessels
N-stage	
NX	Regional lymph nodes cannot be assessed
NO	No regional lymph node metastasis
N1	Regional lymph node metastasis
M-stage	
MX	Distant metastasis cannot be assessed
M0	No distant metastasis
M1	Distant metastasis

termed peptide receptor radionuclide therapy (PRRT), usually employs ^{177}Lu or ^{90}Y, both β-emitters, to label DOTATATE or DOTATOC. A prerequisite for PRRT is that the tumor adequately expresses SSR, as assessed by SSR scintigraphy [13,14].

This review focuses on the currently available anatomical (computed tomography [CT], magnetic resonance imaging [MRI], and ultrasound [US]) and functional (scintigraphy and positron emission tomography [PET]) imaging modalities and their applications in tumor detection and staging as well as in choice of therapy, imaging follow up and prediction of response, with emphasis on the recent developments in imaging.

Imaging techniques

CT

CT is the "work-horse" in the imaging of PNETs. In modern equipment, multiple parallel detector rows (multidetector CT, MDCT), and a quickly rotating X-ray tube enable scanning of both the thorax and the abdomen within a breath-hold. Because of the short scanning time, breathing artifacts can be minimized and the use of iodinated contrast agents may be optimized, according to well-defined imaging protocols [14].

For MDCT of PNETs, the upper abdomen is examined before and after the intravenous administration of an iodinated contrast agent, in the late arterial (or portal-venous inflow) phase, and the whole abdomen in the venous (or portal-venous) phase (triple-phase CT). The early arterial phase is usually not necessary in the preoperative planning, as the arterial anatomy and the relationship of the vessels to the tumor may sufficiently be evaluated in the late arterial phase [14]. The acquired 1 mm, or even sub-mm, images are reconstructed into thicker (3-5 mm) overlapping two-dimensional (2D) images in the transaxial (transversal), coronal and sagittal planes (Multi-Planar Reformats, MPRs). If needed, e.g. to depict vascular anatomy, three-dimensional (3D) maximum intensity projection and volume rendering technique images can easily be reconstructed from the same data set.

Recent technological advances in hard- and software have allowed for quantification of organ and tissue perfusion characteristics by applying CT perfusion technique (dynamic contrast-enhanced CT, DCE-CT). Parameters such as blood flow (BF; defined as the flow rate via the vascular network in a tissue or organ), blood volume (BV; defined as the volume of blood passing through the vascular network in a tissue or organ), mean transit time (MTT; defined as the time needed to flow from an artery to vein), and permeability-surface area product (PS; defined as the flux from plasma to interstitium) can be calculated to add potentially valuable information regarding the hemodynamic characteristics of tumors and organs in a defined bodily region [15]. More specifically, BF may be used as an indicator of vascularity/tumor grade, BV an indicator of vascularity, MTT an indicator of perfusion pressure, and, finally, PS an indicator of immature leaky vascularity [15]. Furthermore, with the advent of dual-energy CT (DECT), it is possible to examine an area of the body by using two different energy levels (i.e. 80 and 140 kVp) instead of a single-energy level as used by conventional MDCT. In that way, materials that exhibit differences in molecular composition can be differentiated from each other and a variety of data sets are obtained (such as iodinated attenuation maps, monochromatic images at various energy levels, virtual unenhanced images) adding useful tissue information [16].

MRI

Compared to CT, the superior soft tissue contrast resolution of MRI, i.e. the ability to distinguish various structures based on their different signal intensity (SI) characteristics, makes it advantageous for the investigation of PNETs. Drawbacks are the limited availability and prolonged image acquisition time compared to CT.

Similarly to contrast-enhanced CT, MRI sequences are obtained before and after the intravenous administration of gadolinium-based chelates in late arterial, portal venous, and, additionally, equilibrium phases [14]. The sequences used for the DCE imaging are preferably fat-saturated 3D T1-weighted and can be primarily obtained in any plane, preferably the transaxial (transversal), with a slice thickness varying from 1.5-4 mm, optimally 2-3 mm. The possibility to reformat preliminary acquired transaxial images to the coronal and sagittal planes (MPRs) exists but the results are not of as high quality as compared to the MPRs at CT examinations due to the lower spatial resolution. The protocol should also include magnetic resonance cholangiopancreatography and T2-weighted sequences (preferably with fat saturation) in order to depict the relation of the lesion(s) to the main pancreatic duct (MPD) and common bile duct (CBD). Organ-specific intravenous contrast agents accumulated in the normal liver parenchyma are valuable for detection and characterization of liver lesions [17].

Diffusion-weighted imaging (DWI) is a relatively new sequence implemented in abdominal applications. It is based on the random translational movement of free water molecules (or Brownian motion), restricted when the extracellular space is diminished, such as when there is tumor-related hypercellularity and/or presence of fibrosis. By calculating the apparent diffusion coefficient (ADC), it is possible to obtain objective measurement of the diffusivity in a given tissue, organ or tumor [18]. Various models for ADC calculations are clinically available today. On the one hand, the automated monoexponential model is easier and faster but combines the microscopic perfusion and diffusion in the acquired measurement rendering it more inaccurate. On the other hand, the biexponential (intravoxel incoherent motion, IVIM) model is of greater complexity but it is able to separate microcirculation in the capillary bed from pure diffusion, which makes it more accurate. Besides ADC calculations, IVIM model allows for the extraction of additional parameters, such as the slow component of diffusion (D_{slow}; representing perfusion-free molecular diffusion), the incoherent microcirculation -or otherwise pseudodiffusion- (D_{fast}; representing microcapillary perfusion) and the perfusion fraction (*f*) [19].

Current magnets have field strengths of either 1.5 or 3 Tesla and allow for DCE-MRI within reasonable time frames (one breath-hold).

Similar to CT, MRI-perfusion technique has been recently made available in advanced scanners [20]. The most important quantitative perfusion parameters that can be extracted from MRI perfusion are the volume transfer coefficient (K^{trans}) between the plasma and the extracellular extravascular space (EES) and the volume of EES per unit tissue (v_e), as described by the bidirectional dual-compartment Toft model [21]. The parameter K^{trans} is related to vessel permeability and BF while v_e is a marker for cell density. However, MRI perfusion is technically much more demanding than its CT counterpart and it suffers from low reproducibility due to many different sources of ambiguity including an adequate definition of arterial input function and an accurate transformation of measured SIs to contrast concentration [21].

US

There are various approaches to US of PNETs such as conventional transabdominal US, endoscopic US (EUS, by inserting a transducer via the endoscope), and intraoperative US (through direct contact of the transducer with the organ surface during surgery). Similar to MRI, US is advantageous in that it does not expose the patient to potentially harmful ionizing radiation, allows for a real-time dynamic examination of the organ of interest and by DCE examination, tissue characterization may be performed based on the in- and outflow pattern of intravenously injected microbubbles [22,23]. Finally, US provides guidance of the biopsy needle for both fine-needle aspiration for cytology and core biopsy for histopathological examination.

General drawbacks with US include the high operator dependency, and that optimal demonstration of image findings to the clinician may be difficult. Transabdominal US is generally less suitable for obese patient. The availability of EUS is generally limited and its results are somehow worse in cases of tumors located in the tail or in ectopic tumors [24].

Nuclear medicine imaging

Nuclear medicine imaging is generally helpful in the imaging work-up of PNETs by scintigraphy using a γ-camera or PET using a PET camera. Current cameras are usually combined with a CT scanner for hybrid imaging and combinations with MRI (PET/MRI) has recently also evolved.

Scintigraphy

The prevailing nuclear medicine NET imaging technique is SSR scintigraphy using radiolabeled SSA, based on the high SSR expression in most neuroendocrine tumors [25]. Octreotide is the most frequently used SSA and is commercially available as ^{111}In-pentetreotide (^{111}In-DTPA-octreotide, Octreoscan™).

By scintigraphy using Octreoscan™ the acquisition is performed as a 2D whole-body examination (anterior and posterior planar imaging) and 3D SPECT (single-photon emission CT) transversal images. Planar imaging is generally performed at 4 h and 24 h after injection, and SPECT at 24 h. Because the SSR expression of benign insulinomas is low or lacking, the detection rate for these is poor.

PET

In PET, the most frequently used radionuclides are ^{18}F, ^{11}C, ^{68}Ga, ^{15}O with generally short half-lives (2-110 min). Compared to scintigraphy, the spatial resolution is better, approximately 0.5 cm for PET and 1.5 cm for SPECT, and image acquisition is generally faster. Drawbacks include the need for a cyclotron to generate most of the PET tracers and the generally more complicated radiochemistry.

For PNET imaging, principally two types of radiotracers are used: those related to receptor expression and those reflecting tumor metabolism [26]. The first category includes SSAs labeled with the positron emitter ^{68}Ga and the most often used preparations are ^{68}Ga-DOTATOC, ^{68}Ga-DOTANOC and ^{68}Ga-DOTATATE. These three exhibit some differences in their affinity to the SSR subtypes 2, 3 and 5, which, however, have not convincingly been shown significant for neuroendocrine tumor imaging in the clinical practice. ^{68}Ga is eluded from a generator, similar to the production of ^{99m}Tc for scintigraphy. Image acquisition can be done within 1 h from injection of the radiotracer and apart from the better spatial resolution, compared to SSR scintigraphy with SPECT, the soft tumor-to-tissue contrast is much higher and allows for imaging of 0.5 cm tumors. Compared to the SSAs used in scintigraphy, ^{68}Ga-SSAs for PET-imaging still have less availability.

The second tracer category for neuroendocrine tumor PET-imaging comprises amine precursors, such as ^{11}C-5-hydroxytryptophan (^{11}C-5-HTP), ^{18}F-DOPA and ^{11}C-L-DOPA, and the glucose analog ^{18}F-FDG. ^{18}F-FDG is by far the most widely available and well-studied PET-tracer in general oncology. For many years, it was regarded unfit for neuroendocrine tumor imaging, except for G3 tumors but recent data show that ^{18}F-FDG may add valuable information to SSA-imaging.

While the amine precursors ^{18}F-DOPA and especially ^{11}C-5-HTP are considerably less available and are used only in specialized centers, they are valuable as problem-solving tools when the suspected tumors are expected to have low or no SSR expression.

Hybrid imaging

In modern scanners, PET and SPECT are combined with an anatomical cross-sectional counterpart such as CT (PET/CT and SPECT/CT) and, lately, also MRI (PET/MRI). In that way, software "fusion" images, for correlation of anatomical and functional findings are additionally available to facilitate the evaluation. With PET/CT and SPECT/CT, CT data are additionally used for attenuation correction of the PET and SPECT images. To fully utilize the diagnostic capacity of PET/CT, it is preferred to perform the CT examination according to dedicated contrast-enhanced CT protocols.

For scintigraphy and PET -as a group- using radiolabeled SSA, the term SSA-imaging will be used in the following text.

Applications

Primary tumor detection

The detection of a functioning PNET can be a diagnostic challenge, as these tumors can cause very prominent hormonal symptoms but may still be small. By contrast, symptoms from non-functioning PNETs are usually secondary to mass-effect (such as abdominal pain, jaundice, weight loss) or due to metastatic disease. Patients with non-functioning PNETs, therefore, more often present with larger tumors that generally are more easily detected, compared to their functioning counterparts.

For reasons of availability, CT and MRI are usually the preferred modalities for the initial investigation. Because of their hypervascular nature, PNETs exhibit robust contrast-enhancement in the late arterial phase, which is therefore the optimal vascular phase for their identification (Fig. 1). In the differential diagnosis, PNETs have to be distinguished from other hypervascular lesions, such as primary exocrine tumors (e.g. serous cystic adenoma, solid pseudopapillary neoplasia, acinar cell carcinoma), hypervascular metastases (e.g. renal cell carcinoma, carcinoid, medullary thyroid carcinoma), neurogenic tumors (e.g. Schwannoma), vascular lesions (e.g. aneurysm, pseudoaneurysm, arteriovenous malformation) and developmental lesions (e.g. intrapancreatic splenule) [27]. However, PNETs do not always exhibit hypervascularity and this is more often the case for non-functioning tumors (Fig. 2) [28]. On unenhanced fat-suppressed T1-weighted sequences, PNETs have lower SI compared to the adjacent parenchyma while on T2-weighted sequences they exhibit more often high SI, although intermediate or low SI may also be observed [28]. In case of cystic degeneration/necrosis, the lesions have low attenuation on unenhanced CT, very high SI on T2-weighted images and thickened contrast-enhancing walls, and may thus resemble cystic pancreatic lesions, such as intraductal papillary mucinous neoplasms, mucinous cystic neoplasm or even pseudocysts [28,29]. Calcifications seem to be somewhat more frequent in non-functioning tumors and are found in approximately every 6th patient with PNET (Fig. 1) [30]. The sensitivity and specificity for CT to localize a PNET is reported to vary between 63-82% and 83-100% [31-36], respectively, whereas the detection rate ranges between 39-94% [29,36-42]. Promising results for the preoperative detection of insulinomas have been reported with the use of dual-energy CT, where the combined use of monochromatic images and iodine maps had a sensitivity of 96% compared to 69% when conventional MDCT was used [43]. The corresponding, sensitivity and specificity for MRI varies between 85-100% and 75-100%, respectively [44,45]; the detection rate for MRI is between 50-94% [37,40,42,46,47].

In a recent report on patients with G1 and G2 PNETs, the detection rate for DWI (visual assessment) was similar to that of contrast-enhanced MRI, in both a lesion-based and a patient-based analysis (Fig. 1, 3) [48]. This is particularly valuable when intravenous administration of MRI contrast agents is contraindicated, e.g. in patients with renal insufficiency or prior allergic reactions to gadolinium chelates. In the same situation, IVIM-derived DWI parameters, such as perfusion fraction (*f*) and incoherent microcirculation D_{fast} can be helpful in differentiating PNETs from pancreatic adenocarcinoma as both parameters have been shown to be significantly higher in PNETs than in adenocarcinomas [49].

If the initial investigation fails to depict the PNET, EUS or SSA-imaging may be applied. The method of choice is highly dependable on the local availability and expertise. EUS has been shown to be the most sensitive technique to visualize PNETs with approximately 90% detection rate (Fig. 1, 4) [36,49-53]. For insulinomas, the sensitivity of EUS is lower than for other PNETs (84 and 92%, respectively) [50]. For PNETs, the sensitivity of Octreoscan™ ranges between 46-93% [54].

Similar to EUS, the sensitivity of Octreoscan™ to visualize insulinomas is somehow lower (50-60%) compared to that for gastrinomas, glucagonomas, VIPomas and non-functioning PNETs (75-100%), which can be attributed to their small size and low expression of SSR (Fig. 4) [55]. For benign insulinomas, scintigraphy with GLP-1 analogs (exendin-3 and -4) has shown promising initial results [56-58].

Within the SSA-imaging group, it is shown in multiple comparative studies that ^{68}Ga-DOTA-SSA PET/PET-CT performs better than Octreoscan™ (Fig. 5) [25]. Regarding which of the three available ^{68}Ga-DOTA tracers should be used in clinical practice (i.e., DOTATOC, DOTANOC, and DOTATATE), published data indicate that there may

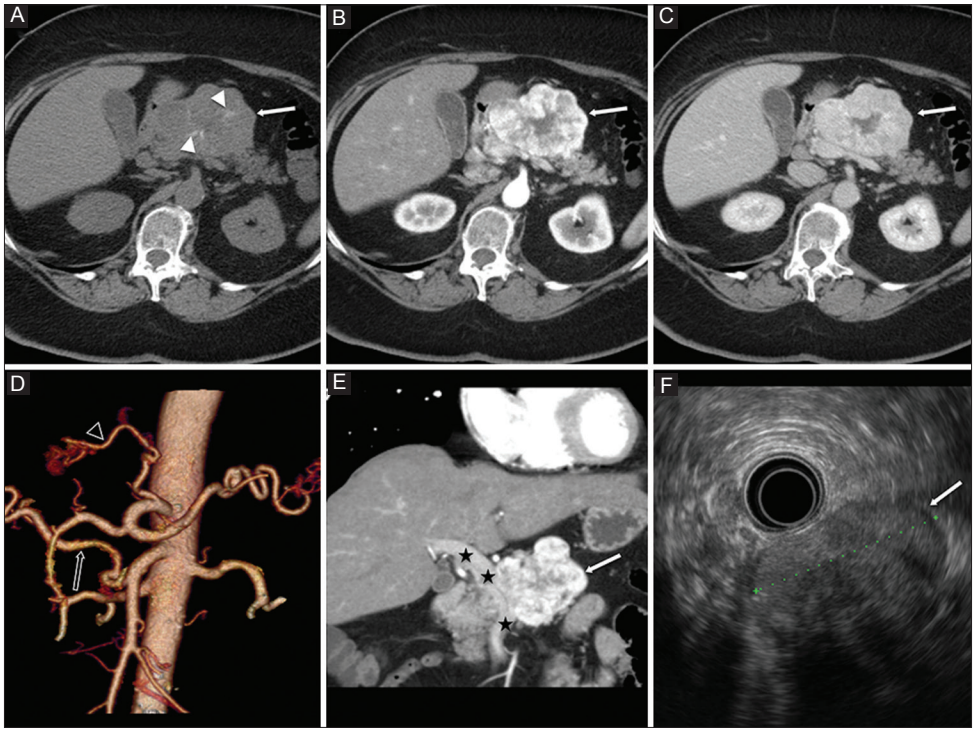

Figure 1 Dedicated computed tomography (CT) examination of a patient presenting with upper abdominal pain showing a pancreatic neuroendocrine tumor (PNET) (white arrow) with typical appearance. On the axial, unenhanced CT image (A), the tumor contains calcifications (white arrowheads), while in the late arterial (B) and portal venous (C) phase of the dynamic contrast imaging, it exhibits early strong enhancement and an area of central necrosis. On the 3D volume-rendered image (D), there is a vascular anatomical variant with the right hepatic artery (open white arrow) originating from the superior mesenteric artery and the artery to the liver segments 2 and 3 (open white arrowhead) originating from the left gastric artery. On the coronal oblique reformat (E), the relation of the tumor to the portal/superior mesenteric vein (black asterisks) can easily be appreciated. On endoscopic ultrasound (F), the tumor is well defined, hypoechoic and slightly heterogenous

be advantages with one preparation for some patients and with another one for other subjects, but that there are no fundamental differences between them for the daily routine imaging. In centers performing PRRT, ^{68}Ga-DOTATATE is generally used for PET/CT before ^{177}Lu-DOTATATE therapy whereas ^{68}Ga-DOTATOC is generally preferred for imaging in centers using ^{90}Y-DOTATOC for PRRT.

In a comparative study on ^{11}C-5-HTP-PET, ^{18}F-DOPA PET and Octreoscan™ for diagnosing PNETs, it was shown that ^{11}C-5-HTP-PET outperformed the other two in both a patient- and a lesion-based analysis. The PET results for all three tracers improved with the addition of CT [59]. However, the results of ^{11}C-5-HTP-PET may be somewhat worse in cases of low differentiated and non-functioning PNETs [60].

When there is a suspicion of a G3 PNET, ^{18}F-FDG is preferred for tumor detection as the SSR expression of these tumors is generally low or missing [26,61,62].

Tumor staging and grading

For the purpose of local staging, it is important to assess the size of the tumor and localization within the pancreas, its relationship to the MPD and CBD, the major peripancreatic vessels (celiac trunk and its branches, superior mesenteric and splenic artery and vein, portal vein) and other adjacent structures (Table 2) [14]. To this end, dedicated CT and/or MRI are preferred due to their higher spatial resolution compared to SSA-imaging by SPECT and PET (Fig. 1, 2, 4); by allowing the assessment of vessel involvement (no involvement, abutment or encasement) as well as the depiction of the precise tumor localization/size and its relationship to the MPD, CT/MRI aid in the decision-making on tumor resectability or not, and in the former case, on which surgical procedure to be undertaken, i.e., enucleation or resection (distal pancreatectomy ± splenectomy and pancreaticoduodenectomy) [63-65]. Notably, it has been reported in two studies that in patients undergoing surgery, preoperative CT/MRI may overestimate vessel involvement [65,66]; however, the CT/MRI technique used in both these two aforementioned studies are not considered "state-of-the-art" by contemporary standards.

Regarding tumor grading, the CT perfusion-extracted parameter BF has been reported to be significantly higher in PNETs G1 than in G2 and G3 tumors [67]. DWI has shown promising results for grading purposes. In G1 tumors, mean ADC values (monoexponential-based calculations) were significantly higher than in G2 and G3 tumors (1.48 and 1.04 x 10^{-3} mm^2/s, respectively); apart from that, G1 tumors exhibited significantly higher ADC

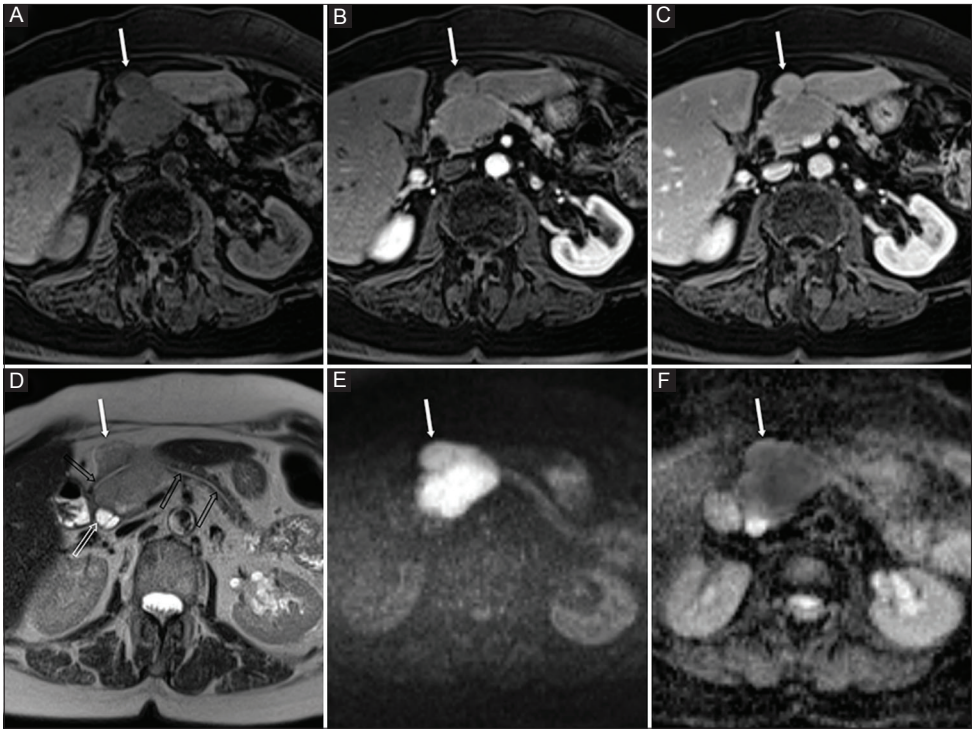

Figure 2 Magnetic resonance imaging examination of a patient complaining for upper abdominal pain, nausea and loss of appetite. On fat-saturated T1-weighted images before (A) and post (B,C) injection of gadolinium chelate, the tumor (white arrow) does not show hypervascularity, a finding that is somehow more common in non-functioning pancreatic neuroendocrine tumors (PNETs). On the T2-weighted HASTE image (D), the tumor shows relatively high SI and its relation to the common bile duct (open white arrow), the main pancreatic duct (open black arrows) and other structures in the area can easily be appreciated. On diffusion image with high b-value (E) and on corresponding apparent diffusion coefficient map (F), there is markedly restricted diffusion. Surgery confirmed a highly-differentiated (G1) PNET

ratios (ADC tumor/ADC pancreas) than G2 and G3 [68]. In the same report, G1 tumors were significantly more often hypervascular, showing contrast-enhancement after intravenous injection of gadoxetic acid, compared to G2 and G3 tumors. Furthermore, Wang *et al* showed that there was a significantly inverse correlation between ADC values and tumor ki-67 index; none of the 14 included G1 PNETs had ADC values (monoexponential-based calculations) lower than 1 x 10^{-3} mm^2/s [69]. MRI perfusion was recently shown to differentiate G1 and G2 from G3 PNETs based on the parameter K^{trans} that is significantly higher in G1 and G2 [70]. Summarizing, CT- and MRI perfusion as well as DWI-based calculations of ADC may be helpful for differentiation of the various grades of PNETs.

CT/MRI of the abdomen and CT of the thorax are generally performed for staging of regional and distant metastases, also in combination with SSA-imaging, which is usually helpful to identify additional metastases in regional and distant lymph nodes, and bone. SSA-imaging is mainly performed by SSR scintigraphy (Octreoscan™) and, lately, with ^{68}Ga-DOTA-SSA PET with increasing frequency [13]. A tumor uptake similar to or higher than that in the normal liver on planar imaging at SSR scintigraphy is in most therapy protocols a prerequisite for PRRT and a positive correlation between the degree of tumor uptake and remission rates has been shown [71]. A high tumor uptake at SSR scintigraphy, however, does not necessarily predict the response to unlabeled ("cold") SSAs that may have a symptomatic effect even when tumor uptake is low.

Therapy monitoring and prediction of response

Cross-sectional morphological imaging by CT and MRI is the mainstay for surveillance and detection of recurrent disease following surgery and locoablative procedures as well as for monitoring of systemic therapies. In younger patients, when multiple examinations over a long time are expected, MRI is to be preferred to decrease radiation dose. For therapy monitoring, the RECIST 1.1 criteria are generally applied whereby the sum of the largest lesion diameters on CT/MRI is registered [72]. Total disappearance of the disease results in complete regression; a decrease by ≥30% compared to the baseline examination results in partial response; and an increase by ≥20% compared to nadir (the examination when the sum of diameters was the smallest) and/or the appearance of new lesions results in progressive disease. When none of these criteria are fulfilled the disease is stable.

Because of the generally low proliferation rate of PNETs, monitoring of changes in tumor size is suboptimal to assess the response to systemic therapies, especially since these tend to stabilize the disease rather than result in tumor shrinkage. This

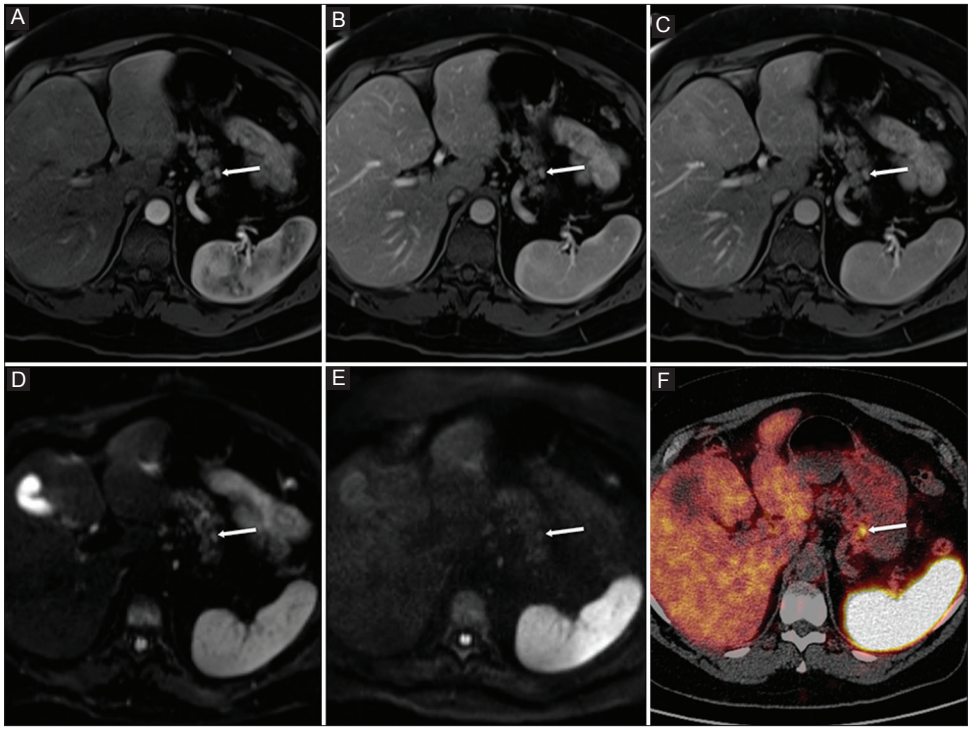

Figure 3 Magnetic resonance imaging (A-E) and ^{68}Ga-DOTATOC positron emission tomography (PET) / computed tomography (CT) (F) examinations of a patient with a small pancreatic neuroendocrine tumor (arrow) located superficially in the distal body/proximal tail area. On the dynamic contrast-enhanced fat-saturated T1-weighted images (A-C), the tumor shows early enhancement. On diffusion-weighted image with low (D) and high b-value (E), the tumor shows discrete restricted diffusion and on 68Ga-DOTATOC PET/CT (F), a distinct high radiotracer uptake in the same area

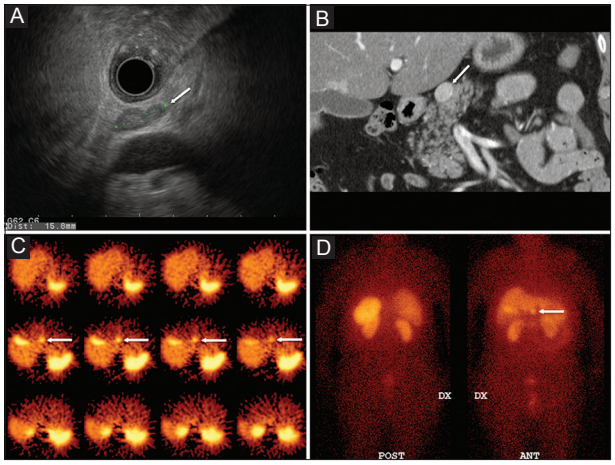

Figure 4 Endoscopic ultrasound (EUS) (A), arterial-phase of the dynamic contrast-enhanced computed tomography (CT) (B) and somatostatin receptor (SSR) scintigraphy with Octreotide (OctreoScan) (C, D) in a patient with a 1.5 cm, accidentally identified hypervascular pancreatic neuroendocrine tumor during CT angiography of the aorta (not shown). All three techniques demonstrate the tumor (arrow); however, the spatial resolution for SSR scintigraphy (C, D) is clearly lower than EUS (A) and CT (B)

holds particularly true for the recent targeted therapies and, therefore, there is a need to develop other response criteria than RECIST. Nuclear imaging techniques are generally helpful to identify new lesions as signs of tumor progression and to characterize lesions that on CT/MRI by conventional morphological size criteria are equivocal. For example, for monitoring of PRRT with ^{177}Lu-DOTATATE it was shown that ^{68}Ga DOTATOC-PET/CT identifies earlier new lesions compared to conventional anatomic imaging [73].

Trials on therapy monitoring of PNETs using nuclear medicine imaging have, however, not been convincing, such as in two PET/CT studies using ^{68}Ga-DOTATOC to monitor PRRT with ^{177}Lu-DOTATATE by measuring changes in the tumor SUV between baseline and follow-up examinations [73,74] There are several problems regarding tumor uptake measurements on ^{68}Ga-DOTA-SSA-PET/CT for therapy monitoring that, at least partly, may explain these results. The amount of administered peptide has been shown to affect both tumor and normal tissue distribution [75]; the injected peptide mass at PET/CT, therefore, needs to be the same at baseline and in the follow-up examinations. The conditions regarding administration of cold SSAs need also to be similar during the time period preceding the baseline and follow-up examinations, respectively. Likewise, in a comparative study on PET/CT with ^{68}Ga-DOTATOC and ^{68}Ga-DOTATATE it was found that the tumor SUV at 1 h did not correlate to the transport rate K_i (according to Patlak) for tumors with SUV>20-25, indicating that SUV does not reflect the SSR expression for tumors with high tracer accumulation [76]. These are two of probably several factors

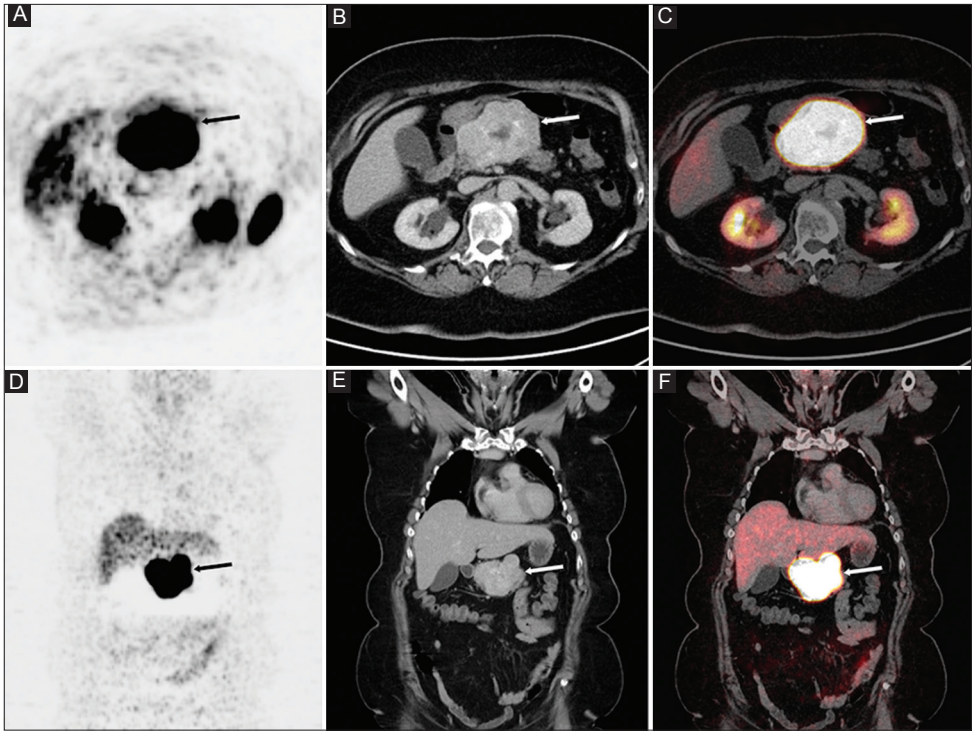

Figure 5 Same patient as in Fig. 1. Images in the axial and coronal plane from ^{68}Ga DOTATOC-positron emission tomography (A,D), portal venous phase of contrast-enhanced computed tomography (B,E) and their fusion (C,F) show very strong radiotracer uptake (SUVmean=70 and SUVmax=184) in this pancreatic neuroendocrine tumor (PNET) (arrow). Surgery confirmed a highly-differentiated (G1) PNET

that may hamper tumor uptake measurements on ^{68}Ga-DOTA-SSA-PET/CT for therapy monitoring.

Therefore, tracers reflecting the metabolic status of the tumor, such as ^{18}F-DOPA and ^{11}C-5-HTP, may be better suited for monitoring response to therapy, independently of the kind of applied treatment. These tracers, however, are still of very limited availability and data from clinical trials do not exist. ^{18}F-FDG-PET/CT is established for therapy monitoring in Medical Oncology and, therefore, may also be applicable in this regard for neuroendocrine carcinomas. In patients with PNETs, ^{18}F-FDG-PET/CT has been shown to predict survival as well as response to PRRT using ^{177}Lu-DOTATATE in G1 and G2 tumors [61,77].

Concluding remarks

A combination of several complementary morphological and nuclear imaging techniques needs to be employed for a number of various applications such as primary PNET detection, assessment of its local invasiveness and relation to adjacent anatomical structures, staging of regional and distant metastases, surveillance for diagnosis of recurrent disease and monitoring of systemic therapies. These examinations need to be performed according to specific protocols but the choice of imaging methods may vary depending on their local availability and expertise. Furthermore, there is a need to develop treatment-response criteria other than RECIST.

References

1. Eriksson B, Oberg K. Neuroendocrine tumours of the pancreas. *Br J Surg* 2000;**87**:129-131.
2. Lam KY, Lo CY. Pancreatic endocrine tumour: a 22-year clinico-pathological experience with morphological, immunohistochemical observation and a review of the literature. *Eur J Surg Oncol* 1997;**23**:36-42.
3. Oberg K. Genetics and molecular pathology of neuroendocrine gastrointestinal and pancreatic tumors (gastroenteropancreatic neuroendocrine tumors). *Curr Opin Endocrinol Diabetes Obes* 2009;**16**:72-78.
4. Antonello D, Gobbo S, Corbo V, Sipos B, Lemoine NR, Scarpa A. Update on the molecular pathogenesis of pancreatic tumors other than common ductal adenocarcinoma. *Pancreatology* 2009;**9**:25-33.
5. Metz DC, Jensen RT. Gastrointestinal neuroendocrine tumors: pancreatic endocrine tumors. *Gastroenterology* 2008;**135**:1469-1492.
6. Massironi S, Sciola V, Peracchi M, Ciafardini C, Spampatti MP, Conte D. Neuroendocrine tumors of the gastro-entero-pancreatic system. *World J Gastroenterol* 2008;**14**:5377-5384.
7. Ehehalt F, Saeger HD, Schmidt CM, Grützmann R. Neuroendocrine tumors of the pancreas. *Oncologist* 2009;**14**:456-467.
8. Rindi G, Arnold R, Bosman FT, et al. Nomenclature and classification of neuroendocrine neoplasms of the digestive system. In Bosman FT, Carneiro F, Hruban RH, Theise ND (eds), WHO classification of tumors of the digestive system, 4th edition. IARC Press: Lyon; 2010, pp. 13-14.
9. Reid MD, Balci S, Saka B, Adsay NV. Neuroendocrine tumors of the pancreas: current concepts and controversies. *Endocr Pathol* 2014;**25**:65-79.
10. Rindi G, Klöppel G, Alhman H, et al. TNM staging of foregut

(neuro) endocrine tumors: a consensus proposal including a grading system. *Virchows Arch* 2006;**449**:395-401.
11. Bilimoria KY, Tomlinson JS, Merkow RP, et al. Clinicopathologic features and treatment trends of pancreatic neuroendocrine tumors: analysis of 9,821 patients. *J Gastrointest Surg* 2007;**11**:1460-7; discussion 1467-1469.
12. Ro C, Chai W, Yu VE, Yu R. Pancreatic neuroendocrine tumors: biology, diagnosis, and treatment. *Chin J Cancer* 2013;**32**:312-324.
13. Bergsma H, van Vliet EI, Teunissen JJ, et al. Peptide receptor radionuclide therapy (PRRT) for GEP-NETs. *Best Pract Res Clin Gastroenterol* 2012;**26**:867-881.
14. Sundin A, Vullierme MP, Kaltsas G, Plöckinger U; Mallorca Consensus Conference participants; European Neuroendocrine Tumor Society. ENETS consensus guidelines for the standards of care in neuroendocrine tumors: radiological examinations. *Neuroendocrinology* 2009;**90**:167-183.
15. Kambadakone AR, Sahani DV. Body perfusion CT: technique, clinical applications, and advances. *Radiol Clin North Am* 2009;**47**:161-178.
16. De Cecco CN, Darnell A, Rengo M, et al. Dual-energy CT: oncologic applications. *AJR Am J Roentgenol* 2012;**199** (Suppl 5):98-105.
17. Albiin N. MRI of Focal Liver Lesions. *Curr Med Imaging Rev* 2012;**8**:107-116.
18. Le Bihan D. Molecular diffusion, tissue microdynamics and microstructure. *NMR Biomed* 1995;**8**:375-386.
19. Koh DM, Collins DJ, Orton MR. Intravoxel incoherent motion in body diffusion-weighted MRI: reality and challenges. *AJR Am J Roentgenol* 2011;**196**:1351-1361.
20. Song HK, Dougherty L. Dynamic MRI with projection reconstruction and KWIC processing for simultaneous high spatial and temporal resolution. *Magn Reson Med* 2004;**52**:815-824.
21. Tofts PS, Brix G, Buckley DL, et al. Estimating kinetic parameters from dynamic contrast-enhanced T(1)-weighted MRI of a diffusable tracer: standardized quantities and symbols. *J Magn Reson Imaging* 1999;**10**:223-232.
22. Badea R, Seicean A, Diaconu B, et al. Contrast-enhanced ultrasound of the pancreas--a method beyond its potential or a new diagnostic standard? *J Gastrointestin Liver Dis* 2009;**18**:237-242.
23. Kitano M, Kudo M, Sakamoto H, Komaki T. Endoscopic ultrasonography and contrast-enhanced endoscopic ultrasonography. *Pancreatology* 2011;**11** (Suppl 2):28-33.
24. Kim MK. Endoscopic ultrasound in gastroenteropancreatic neuroendocrine tumors. *Gut Liver* 2012;**6**:405-410.
25. van Essen M, Sundin A, Krenning EP, Kwekkeboom DJ. Neuroendocrine tumours: the role of imaging for diagnosis and therapy. *Nat Rev Endocrinol* 2014;**10**:102-114.
26. Rufini V, Baum RP, Castaldi P, et al. Role of PET/CT in the functional imaging of endocrine pancreatic tumors. *Abdom Imaging* 2012;**37**:1004-1020.
27. Bhosale PR, Menias CO, Balachandran A, et al. Vascular pancreatic lesions: spectrum of imaging findings of malignant masses and mimics with pathologic correlation. *Abdom Imaging* 2013;**38**:802-817.
28. Herwick S, Miller FH, Keppke AL. MRI of islet cell tumors of the pancreas. *AJR Am J Roentgenol* 2006;**187**:W472-W480.
29. Hammond NA, Miller FH, Day K, Nikolaidis P. Imaging features of the less common pancreatic masses. *Abdom Imaging* 2013;**38**:561-572.
30. Poultsides GA, Huang LC, Chen Y, et al. Pancreatic neuroendocrine tumors: radiographic calcifications correlate with grade and metastasis. *Ann Surg Oncol* 2012;**19**:2295-2303.
31. Stark DD, Moss AA, Goldberg HI, Deveney CW. CT of pancreatic islet cell tumors. *Radiology* 1984;**150**:491-494.
32. Rossi P, Baert A, Passariello R, Simonetti G, Pavone P, Tempesta P. CT of functioning tumors of the pancreas. *AJR Am J Roentgenol* 1985;**144**:57-60.
33. Van Hoe L, Gryspeerdt S, Marchal G, Baert AL, Mertens L. Helical CT for the preoperative localization of islet cell tumors of the pancreas: value of arterial and parenchymal phase images. *AJR Am J Roentgenol* 1995;**165**:1437-1439.
34. Procacci C, Carbognin G, Accordini S, et al. Nonfunctioning endocrine tumors of the pancreas: possibilities of spiral CT characterization. *Eur Radiol* 2001;**11**:1175-1183.
35. Fidler JL, Fletcher JG, Reading CC, et al. Preoperative detection of pancreatic insulinomas on multiphasic helical CT. *AJR Am J Roentgenol* 2003;**181**:775-780.
36. Versari A, Camellini L, Carlinfante G, et al. Ga-68 DOTATOC PET, endoscopic ultrasonography, and multidetector CT in the diagnosis of duodenopancreatic neuroendocrine tumors: a single-centre retrospective study. *Clin Nucl Med* 2010;**35**:321-328.
37. Termanini B, Gibril F, Reynolds JC, et al. Value of somatostatin receptor scintigraphy: a prospective study in gastrinoma of its effect on clinical management. *Gastroenterology* 1997;**112**:335-347.
38. King AD, Ko GT, Yeung VT, Chow CC, Griffith J, Cockram CS. Dual phase spiral CT in the detection of small insulinomas of the pancreas. *Br J Radiol* 1998;**71**:20-23.
39. Stafford-Johnson DB, Francis IR, Eckhauser FE, Knol JA, Chang AE. Dual-phase helical CT of nonfunctioning islet cell tumors. *J Comput Assist Tomogr* 1998;**22**:335-339.
40. Ichikawa T, Peterson MS, Federle MP, et al. Islet cell tumor of the pancreas: biphasic CT versus MR imaging in tumor detection. *Radiology* 2000;**216**:163-171.
41. Gouya H, Vignaux O, Augui J, et al. CT, endoscopic sonography, and a combined protocol for preoperative evaluation of pancreatic insulinomas. *AJR Am J Roentgenol* 2003;**181**:987-992.
42. Shi W, Johnston CF, Buchanan KD, et al. Localization of neuroendocrine tumours with [111In] DTPA-octreotidephy (Octreoscan): a comparative study with CT and MR imaging. *QJM* 1998;**91**:295-301.
43. Lin XZ, Wu ZY, Tao R, et al. Dual energy spectral CT imaging of insulinoma-Value in preoperative diagnosis compared with conventional multi-detector CT. *Eur J Radiol* 2012;**81**:2487-2494.
44. Thoeni RF, Mueller-Lisse UG, Chan R, Do NK, Shyn PB. Detection of small, functional islet cell tumors in the pancreas: selection of MR imaging sequences for optimal sensitivity. *Radiology* 2000;**214**:483-490.
45. Semelka RC, Custodio CM, Cem Balci N, Woosley JT. Neuroendocrine tumors of the pancreas: spectrum of appearances on MRI. *J Magn Reson Imaging* 2000;**11**:141-148.
46. Carlson B, Johnson CD, Stephens DH, Ward EM, Kvols LK. MRI of pancreatic islet cell carcinoma. *J Comput Assist Tomogr* 1993;**17**:735-740.
47. Owen NJ, Sohaib SA, Peppercorn PD, et al. MRI of pancreatic neuroendocrine tumours. *Br J Radiol* 2001;**74**:968-973.
48. Schmid-Tannwald C, Schmid-Tannwald CM, Morelli JN, et al. Comparison of abdominal MRI with diffusion-weighted imaging to 68Ga-DOTATATE PET/CT in detection of neuroendocrine tumors of the pancreas. *Eur J Nucl Med Mol Imaging* 2013;**40**:897-907.
49. Kang KM, Lee JM, Yoon JH, Kiefer B, Han JK, Choi BI. Intravoxel incoherent motion diffusion-weighted MR imaging for characterization of focal pancreatic lesions. *Radiology* 2014;**270**:444-453.
50. Ishikawa T, Itoh A, Kawashima H, et al. Usefulness of EUS combined with contrast-enhancement in the differential diagnosis of malignant versus benign and preoperative localization of pancreatic endocrine tumors. *Gastrointest Endosc* 2010;**71**:951-959.
51. Khashab MA, Yong E, Lennon AM, et al. EUS is still superior to multidetector computerized tomography for detection of pancreatic neuroendocrine tumors. *Gastrointest Endosc* 2011;**73**:691-696.
52. Atiq M, Bhutani MS, Bektas M, et al. EUS-FNA for pancreatic

neuroendocrine tumors: a tertiary cancer center experience. *Dig Dis Sci* 2012;**57**:791-800.
53. Pais SA, Al-Haddad M, Mohamadnejad M, et al. EUS for pancreatic neuroendocrine tumors: a single-center, 11-year experience. *Gastrointest Endosc* 2010;**71**:1185-1193.
54. Koopmans KP, Neels ON, Kema IP, et al. Molecular imaging in neuroendocrine tumors: molecular uptake mechanisms and clinical results. *Crit Rev Oncol Hematol* 2009;**71**:199-213.
55. de Herder WW, Kwekkeboom DJ, Valkema R, et al. Neuroendocrine tumors and somatostatin: imaging techniques. *J Endocrinol Invest* 2005;**28**:132-136.
56. Wild D, Mäcke H, Christ E, Gloor B, Reubi JC. Glucagon-like peptide 1-receptor scans to localize occult insulinomas. *N Engl J Med* 2008 **14**;359:766-768.
57. Christ E, Wild D, Forrer F, et al. Glucagon-like peptide-1 receptor imaging for localization of insulinomas. *J Clin Endocrinol Metab* 2009;**94**:4398-4405.
58. Wild D, Theodoraki A, Kurzawinski TR, et al. Running on empty. *Eur J Nucl Med Mol Imaging* 2010;**37**:1439-1440.
59. Koopmans KP, Neels OC, Kema IP, et al. Improved staging of patients with carcinoid and islet cell tumors with 18F-dihydroxy-phenyl-alanine and 11C-5-hydroxy-tryptophan positron emission tomography. *J Clin Oncol* 2008;**26**:1489-1495.
60. Orlefors H, Sundin A, Garske U, et al. Whole-body (11) C-5-hydroxytryptophan positron emission tomography as a universal imaging technique for neuroendocrine tumors: comparison with somatostatin receptor scintigraphy and computed tomography. *J Clin Endocrinol Metab* 2005;**90**:3392-3400.
61. Binderup T, Knigge U, Loft A, et al. Functional imaging of neuroendocrine tumors: a head-to-head comparison of somatostatin receptor scintigraphy, 123I-MIBG scintigraphy, and 18F-FDG PET. *J Nucl Med* 2010;**51**:704-712.
62. Bhate K, Mok WY, Tran K, Khan S, Al-Nahhas A. Functional assessment in the multimodality imaging of pancreatic neuro-endocrine tumours. *Minerva Endocrinol* 2010;**35**:17-25.
63. Plöckinger U, Rindi G, Arnold R, et al. Guidelines for the diagnosis and treatment of neuroendocrine gastrointestinal tumours. A consensus statement on behalf of the European Neuroendocrine Tumour Society (ENETS). *Neuroendocrinology* 2004;**80**:394-424.
64. Fendrich V, Waldmann J, Bartsch DK, Langer P. Surgical management of pancreatic endocrine tumors. *Nat Rev Clin Oncol* 2009;**6**:419-428.
65. Norton JA, Harris EJ, Chen Y, et al. Pancreatic endocrine tumors with major vascular abutment, involvement, or encasement and indication for resection. *Arch Surg* 2011;**146**:724-732.
66. Hellman P, Andersson M, Rastad J, et al. Surgical strategy for large or malignant endocrine pancreatic tumors. *World J Surg* 2000;**24**:1353-1360.
67. d'Assignies G, Couvelard A, Bahrami S, et al. Pancreatic endocrine tumors: tumor blood flow assessed with perfusion CT reflects angiogenesis and correlates with prognostic factors. *Radiology* 2009;**250**:407-416.
68. Jang KM, Kim SH, Lee SJ, Choi D. The value of gadoxetic acid-enhanced and diffusion-weighted MRI for prediction of grading of pancreatic neuroendocrine tumors. *Acta Radiol* 2014;**55**:140-148.
69. Wang Y, Chen ZE, Yaghmai V, et al. Diffusion-weighted MR imaging in pancreatic endocrine tumors correlated with histopathologic characteristics. *J Magn Reson Imaging* 2011;**33**:1071-1079.
70. Kim JH, Lee JM, Park JH, et al. Solid pancreatic lesions: characterization by using timing bolus dynamic contrast-enhanced MR imaging assessment--a preliminary study. *Radiology* 2013;**266**:185-196.
71. Kwekkeboom DJ, Teunissen JJ, Bakker WH, et al. Radiolabeled somatostatin analog [177Lu-DOTA0,Tyr3] octreotate in patients with endocrine gastroenteropancreatic tumors. *J Clin Oncol* 2005;**23**:2754-2762.
72. Eisenhauer EA, Therasse P, Bogaerts J, et al. New response evaluation criteria in solid tumours: revised RECIST guideline (version 1.1). *Eur J Cancer* 2009;**45**:228-247.
73. Gabriel M, Oberauer A, Dobrozemsky G, et al. 68Ga-DOTA-Tyr3-octreotide PET for assessing response to somatostatin-receptor-mediated radionuclide therapy. *J Nucl Med* 2009;**50**:1427-1434.
74. Haug AR, Auernhammer CJ, Wängler B, et al. 68Ga-DOTATATE PET/CT for the early prediction of response to somatostatin receptor-mediated radionuclide therapy in patients with well-differentiated neuroendocrine tumors. *J Nucl Med* 2010;**51**:1349-1356.
75. Velikyan I, Sundin A, Eriksson B, et al. In vivo binding of [68Ga]-DOTATOC to somatostatin receptors in neuroendocrine tumours-impact of peptide mass. *Nucl Med Biol* 2010;**37**:265-275.
76. Velikyan I, Sundin A, Sörensen J, et al. Quantitative and qualitative intrapatient comparison of 68Ga-DOTATOC and 68Ga-DOTATATE: net uptake rate for accurate quantification. *J Nucl Med* 2014;**55**:204-210.
77. Severi S, Nanni O, Bodei L, et al. Role of 18FDG PET/CT in patients treated with 177Lu-DOTATATE for advanced differentiated neuroendocrine tumours. *Eur J Nucl Med Mol Imaging* 2013;**40**:881-888.